AGU PUBLICATIONS

Geophysical Research Letters

RESEARCH LETTER
10.1002/2016GL068097

Key Points:
- Surface nutrient concentrations in the North Pacific are optimally interpolated
- The PDO- and NPGO- related nutrient variability are presented
- Phosphate and silicate trends are negative, but nitrate shows no trend

Supporting Information:
- Supporting Information S1

Correspondence to:
S. Yasunaka,
yasunaka@jamstec.go.jp

Citation:
Yasunaka, S., T. Ono, Y. Nojiri, F. A. Whitney, C. Wada, A. Murata, S. Nakaoka, and S. Hosoda (2016), Long-term variability of surface nutrient concentrations in the North Pacific, *Geophys. Res. Lett.*, *43*, 3389–3397, doi:10.1002/2016GL068097.

Received 7 FEB 2016
Accepted 15 MAR 2016
Accepted article online 21 MAR 2016
Published online 5 APR 2016

Long-term variability of surface nutrient concentrations in the North Pacific

S. Yasunaka[1], T. Ono[2], Y. Nojiri[3], F. A. Whitney[4], C. Wada[3], A. Murata[1], S. Nakaoka[3], and S. Hosoda[1]

[1]Research and Development Center for Global Change, Japan Agency for Marine-Earth Science and Technology, Yokosuka, Japan, [2]National Research Institute of Fisheries Science, Fisheries Research Agency, Yokohama, Japan, [3]Center for Global Environmental Research, National Institute for Environmental Studies, Tsukuba, Japan, [4]Institute of Ocean Sciences, Fisheries and Oceans Canada, Ottawa, Ontario, Canada

Abstract We present the spatial distributions and temporal changes of the long-term variability of surface nutrient concentrations in the North Pacific by using nutrient samples collected by volunteer ships and research vessels from 1961 to 2012. Nutrient samples are optimally interpolated onto 1° × 1° monthly grid boxes. When the Pacific Decadal Oscillation is in its positive phase, nutrient concentrations in the western North Pacific are significantly higher than the climatological means, and those in the eastern North Pacific are significantly lower. When the North Pacific Gyre Oscillation is in its positive phase, nutrient concentrations in the subarctic are significantly higher than the climatological means. The trends of phosphate and silicate averaged over the North Pacific are $-0.012 \pm 0.005\ \mu mol\ l^{-1}\ decade^{-1}$ and $-0.38 \pm 0.13\ \mu mol\ l^{-1}\ decade^{-1}$, whereas the nitrate trend is not significant ($0.01 \pm 0.13\ \mu mol\ l^{-1}\ decade^{-1}$).

1. Introduction

One response to global warming has been warming and freshening of the mixed layer of the ocean, both of which should reduce the transport of nutrients to the euphotic zone [*Woods and Barkmann*, 1993; *Bopp et al*., 2001]. Trends toward shallower mixed layer depths and lower nutrient concentrations have been reported in several regions of the subarctic North Pacific [*Freeland et al*., 1997; *Ono et al*., 2002, 2008]. The decrease of nitrate has been less prominent than the decreases of phosphate and silicate in the North Pacific subpolar region [*Watanabe et al*., 2008] and the western North Pacific [*Kim et al*., 2011]. Increasing atmospheric nitrogen deposition has been considered as one explanation for the nitrate less prominent trend [*Duce et al*., 2008; *Kim et al*., 2011]. Decadal variations in upper ocean nutrient concentrations have also been reported in the North Pacific [*Peña and Varela*, 2007; *Di Lorenzo et al*., 2009; *Yasunaka et al*., 2014]. However, these earlier studies were conducted over small areas or for short periods of time; spatiotemporal features of long-term variability in the whole North Pacific have not been identified.

The National Institute for Environmental Studies (NIES, Japan) and the Institute of Ocean Science (IOS, Canada) have carried out surface nutrient sampling from a ship of opportunity in the North Pacific [*Whitney*, 2011; *Yasunaka et al*., 2014]. Ship-of-opportunity observations provide better data coverage than bottle sampling by research vessels. In this study, we use both ship-of-opportunity observations and bottle samples collected by research vessels to elucidate spatial patterns and temporal changes in the long-term variability of surface nutrient concentrations from 1961 to 2012.

2. Data and Methods

2.1. Discrete Water Samples for Nutrients

We use surface samples of nutrients (phosphate, nitrate, and silicate) collected by the NIES and IOS. We also include nutrient concentrations measured by the Japan Agency for Marine-Earth Science and Technology (JAMSTEC) surface nutrient monitoring system, nutrient concentrations from bottle samples collected along Line P by the IOS, and data archived in the PACIFic ocean Interior CArbon (PACIFICA) database and World Ocean Database 2013 (WOD13). The total number of measurements is about 82,000 (Figure 1).

The NIES has carried out ship-of-opportunity sampling from volunteer ships since 1995 [*Yasunaka et al*., 2014]. Surface samples (depths of 5–10 m) were manually collected and stored frozen; the nutrients were then analyzed in onshore laboratories. The NIES analyzed about 9000 surface nutrient samples collected from widely distributed locations in the North Pacific. The IOS also carried out ship-of-opportunity surface

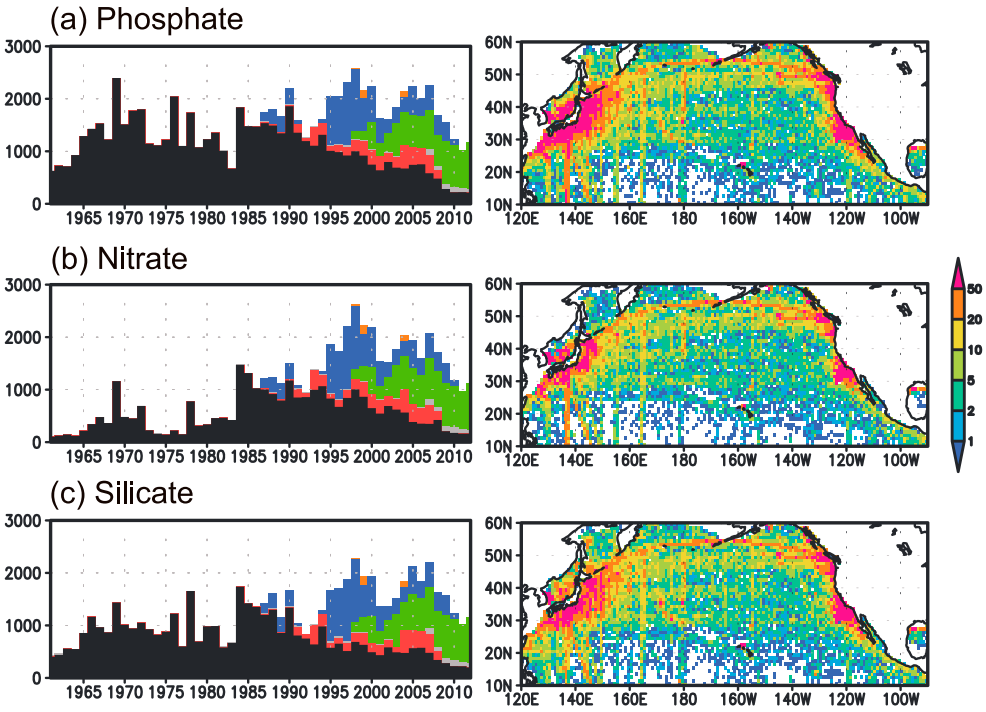

Figure 1. (a (left) to c (left)) Temporal (black, WOD; red, PACIFICA; gray, Line P; green, NIES; blue, IOS; and orange, JAMSTEC monitoring) and (a (right) to c (right)) spatial distribution of nutrient samples in the North Pacific from 1961 to 2012 for (a) phosphate, (b) nitrate, and (c) silicate.

sampling (depths of 5−10 m) mainly in the subarctic region from 1987 to 2010 [*Whitney*, 2011]; approximately 10,000 samples were collected. The detection limits of the NIES and IOS samples are 0.02 μmol l^{-1} for phosphate, 0.1 μmol l^{-1} for nitrate, and 0.6 μmol l^{-1} for silicate (Y. Nojiri and F. A. Whitney, personal communications, 2015).

Nutrient monitoring was performed on the JAMSTEC research vessel *Mirai* from 1998 to 2004 (cruises MR98-02, MR99-07, MR04-E04, and MR04-05). Seawater from a depth of 4 m was pumped to the shipboard laboratory and introduced directly into a continuous monitoring system (Bran + Luebbe Model TRAACS 800) through a narrow tube. Monitoring data were obtained every minute and calibrated every 12 h. We average the nutrient data on a daily basis within 1° latitude × 1° longitude grid boxes. There are about 300 grid boxes of averaged data from the JAMSTEC monitoring.

The PACIFICA database contains nutrient data from research vessels in the Pacific spanning the period 1997−2008 [*Suzuki et al.*, 2013]. On Line P surveys, samples have been collected since 1956 at 27 oceanic stations from near the coast of southern British Colombia to 50°N, 145°W in the North Pacific eastern subarctic [*Fisheries and Oceans Canada*, 2012]. We extract values from the shallowest depths in the upper 20 m of each cast in the PACIFICA and Line P databases. The PACIFICA and Line P databases include approximately 4000 and 900 nutrient samples, respectively. We also use the nutrient samples at a standard depth of 10 m archived in the WOD13 [*Boyer et al.*, 2013]. There are approximately 58,000 nutrient samples from WOD13 in the North Pacific from 1961 to 2012, although most of the data were collected in regions offshore of North America and around Japan. Duplicates with data archived in PACIFICA and the Line P data set are excluded from WOD13. The NIES, IOS, and JAMSTEC observations are not included in WOD13.

The locations of the nutrient samples are spread widely over the North Pacific, although many of them are concentrated around Japan, near the North American coast, and along several fixed lines and main routes of volunteer ships (Figures 1a (right) to 1c (right)). The numbers of phosphate and silicate samples are similar throughout the analysis periods, but the number of nitrate samples is low before the 1980s (Figures 1a (left) to 1c (left)). Nutrient samples are collected in all seasons, although there are slightly fewer data in autumn than in the other seasons, especially before the start of the ship-of-opportunity programs (Figure S1 in the supporting information).

2.2. Optimal Interpolation of the Nutrient Concentrations

We use the same methodology as *Yasunaka et al.* [2014] to perform statistical checks on the surface nutrient data. As reference values, we use long-term mean (i.e., climatology) and standard deviations in a window for phosphate, nitrate, and silicate, respectively. We eliminate data that are more than 3 standard deviations from the climatology. This procedure is iterated four times while gradually reducing the window size; the sizes for longitude, latitude, and month are (±30°, ±10°, ±2), (±10°, ±5°, ±2), (±10°, ±5°, ±1), and (±5°, ±2°, ±1) in turn. The size of the smallest window is set so that the number of data in the window is at least 100. Consequently, we exclude about 3000 measurements (4% of the total) as erroneous or extreme data for our large-scale analysis. Finally, we average the remaining measurements onto 1° × 1° monthly grid boxes for each year from 1961 to 2012 for phosphate, nitrate, and silicate. We designate these data as the quality-controlled monthly data.

Next, we calculate autocorrelation functions of the climatological monthly means of the quality-controlled data to identify the decorrelation radius and signal-to-noise ratio (Figure S2). The autocorrelation functions for phosphate, nitrate, and silicate are similar to each other. Because the autocorrelation functions cross zero from 16° to 22° in the meridional direction, from 21° to 24° in the zonal direction, and at 3 months in time, we set the decorrelation radius to ±20° in latitude, ±23° in longitude, and ±3 months. Gaps of autocorrelations in space between lag 0 and lag 1 average 0.6. The signal-to-noise ratio is therefore set to 1.5 [= 0.6/(1 − 0.6)].

We then adopt optimal interpolation for the quality-controlled monthly data with the decorrelation radius and signal-to-noise ratio mentioned above. We use the 10 year mean of nutrient concentrations presented by *Yasunaka et al.* [2014] as the first guess. Window sizes for calculation of covariance matrices are set to be twice the size of the decorrelation radius. *Hosoda et al.* [2008] presented detailed equations for optimal interpolation.

In our calculations described in section 3, we use interpolated results in cases where the interpolation square error ratios are less than 0.7 because optimal interpolation results with square error ratios more than 0.7 tend to be the first guesses. We omit estimated concentrations lower than 0.02 μmol l^{-1} for phosphate, 0.1 μmol l^{-1} for nitrate, and 0.6 μmol l^{-1} for silicate which are the detection limits of the NIES and IOS samples. As a result, each 1° × 1° grid box in most of the North Pacific, except for the central region south of 25°N, contain more than 30 data points for each nutrient during the period 1961 to 2012. We use those time series in the following analyses.

2.3. Other Gridded Data Sets

Ocean temperature and salinity data are taken from *Ishii and Kimoto* [2009]. Their data set has a 1° × 1° (latitude × longitude) spatial and a monthly temporal resolution, with 24 vertical levels in the upper 1500 m. Sea surface density is calculated from sea surface temperature (SST) and sea surface salinity by *Ishii and Kimoto* [2009]. Surface wind data are taken from the National Centers for Environmental Prediction/National Center for Atmospheric Research Reanalysis 1; those data have a 2.5° × 2.5° spatial and a monthly temporal resolution [*Kalnay et al.*, 1996].

We use climatological means of mixed layer depths (MLDs) from the monthly climatology produced by JAMSTEC (MILA_GPV) [*Hosoda et al.*, 2010]. We fill missing MLDs at individual grid points with the average of data in the surrounding grid points. We use climatological means of euphotic zone depths from MODIS ocean color measurements reported by *Lee et al.* [2007]. We also use monthly nutrient climatology from the World Ocean Atlas 2013 (WOA13) [*Garcia et al.*, 2014].

2.4. Decomposition Method

The Pacific Decadal Oscillation (PDO) and North Pacific Gyre Oscillation (NPGO) are the two dominant modes of low-frequency climate variability in the North Pacific [*Mantua et al.*, 1997; *Di Lorenzo et al.*, 2008]. To detect nutrient variations associated with the PDO, the NPGO, and the linear trend, the PDO index, the NPGO index, and the linear trend time series are multiply regressed on the nutrient anomalies in each grid (Figure 2). We define the linear trend time series as a constant increasing sequence at the rate of 1 decade^{-1}. The PDO index, the NPGO index, and the linear trend time series are not significantly

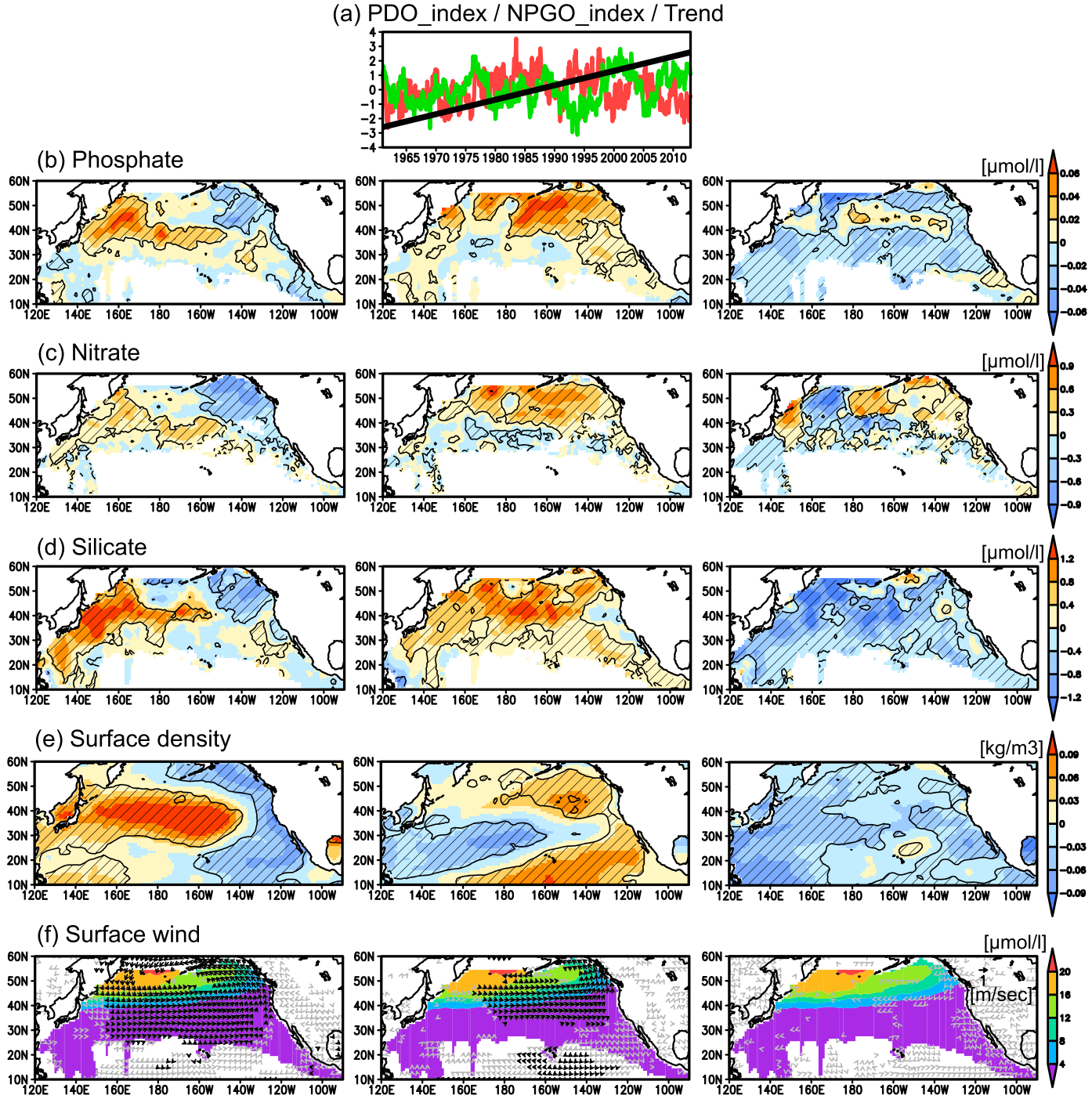

Figure 2. (a) PDO index (red), NPGO index (green), and linear trend time series (black). (b) Phosphate, (c) nitrate, (d) silicate, (e) surface density, and (f) surface wind ($p < 0.05$; black arrows denote |regression vector| > 0.1 m s^{-1}) multiple regression patterns onto the (Figures 2a (left) to 2f (left)) PDO index, the (Figures 2a (middle) to 2f (middle)) NPGO index, and the (Figures 2a (right) to 2f (right)) linear trend time series. Shaded areas indicate regression coefficients significant at $p < 0.05$. Colored shadings in Figure 2f show climatological annual means of nitrate concentrations.

correlated with each other during the analysis period. A multiple linear regression equation with three variables is represented as follows:

$$Y = b_1 \times X_1 + b_2 \times X_2 + b_3 \times X_3 + \varepsilon. \quad (1)$$

In equation (1), the nutrient concentration anomaly from long-term monthly mean is Y, and the PDO index, NPGO index, and linear trend time series are X_1, X_2, and X_3, respectively. Values of b_1, b_2, and b_3 (the partial

regression coefficients) are found by minimizing the sum of the squares of the ε values (the residuals; the deviations between the expected and observed values of Y). The first three terms in equation (1) explain 20−27% of the total variance of the nutrient concentrations. These percentages are comparable to the percentage of the SST variance explained by the same three variables (25%). Month-to-month differences of regression patterns are not considered here (the multiple regression explain 50% of the SST variance if we calculate equation (1) for each month and then determined the explained variance).

We also conduct many sensitivity tests of the multiple regression analyses. To examine the effect of differences of spatial coverage, we resample phosphate and silicate data only in the grids where there are nitrate data (data coverage of nitrate is the most limited of the three nutrients) and apply regression analyses to the resampled phosphate and silicate data. To investigate seasonal dependency, we apply regression analyses to data in each month. To examine discrepancies between data sources, we apply regression analyses to data from the WOD, PACIFICA, and Line P data sets (i.e., bottle samples) and to those from the NIES, IOS, and JAMSTEC monitoring data sets (i.e., underway samplings).

We also apply multiple regression analyses to the surface density and surface wind data to examine how the PDO, NPGO, and linear trends affect nutrient variability by changing physical conditions. Changes of surface density are closely related to changes of the mixed layer depth (e.g., lower density is associated with a shallower mixed layer depth). Changes of surface winds induce changes of horizontal advection via Ekman transport (e.g., a westerly wind anomaly induces southward Ekman transport in the Northern Hemisphere).

3. Results

3.1. Variability Related to the Pacific Decadal Oscillation

When the PDO is in its positive phase, nutrient concentrations in the western North Pacific are significantly higher than the climatological mean values, and those in the eastern North Pacific are significantly lower (Figures 2b (left) to 2d (left)). Regression patterns of the three nutrients are similar to each other, and the ratios of the regression coefficients of each nutrient are approximately consistent with Redfield stoichiometry. The results of the sensitivity tests reveal that all regression patterns associate with the PDO are similar to each other, and spatial correlations between regression patterns obtained by using all the data and those from the sensitivity tests are all significant ($p < 0.05$; degrees of freedom = number of grid points/decorrelation radius for the optimal interpolation).

The signs of the changes of nutrient concentrations associated with the PDO are generally the same as the signs of surface density changes throughout the North Pacific (Figure 2e (left)). When the PDO is in its positive phase, the density is greater, implying that the SST is lower and the mixed layer deeper in the western Pacific, as a result of the intense, dry, and cold wind from the Asian continent [*Cayan*, 1992; *Miller et al*., 1994]. At the same time, higher SSTs and shallower mixed layers (i.e., water with a lower density) are found in the eastern North Pacific, which corresponds to the anomalous southerly winds as reported by *Cayan* [1992] and *Miller et al.* [1994]. A deepening (shoaling) of the mixed layer would induce an increase (decrease) of nutrient concentrations via enhanced (weakened) entrainment of subsurface, nutrient-rich water. Wind changes associated with the PDO also induce changes in horizontal advection. When the PDO is in its positive phase, intense westerly winds force more nutrient-rich water southward from the subarctic to midlatitudes (Figure 2f (left)).

3.2. Variability Related to the North Pacific Gyre Oscillation

When the NPGO is in its positive phase, nutrient concentrations in the subarctic are significantly higher than climatology (Figures 2b (middle) to 2d (middle)). The regression patterns of the three nutrients are similar to each other, and the ratios of the regression coefficients of the nutrients are approximately consistent with Redfield stoichiometry. All regression patterns associate with the NPGO in the sensitivity tests are similar to each other, and spatial correlations between the regression patterns obtained by using all the data and those from the sensitivity tests are all significant.

The signs of the changes of nutrient concentrations associated with the NPGO are generally the same as the signs of the changes of surface density in the subarctic (Figure 2e (middle)). When the NPGO is in its positive phase, the density is greater, the SST is lower, and the mixed layer is deeper; this pattern can be explained by the intense horizontal advection associated with the westerly wind anomaly that occurs in the subarctic

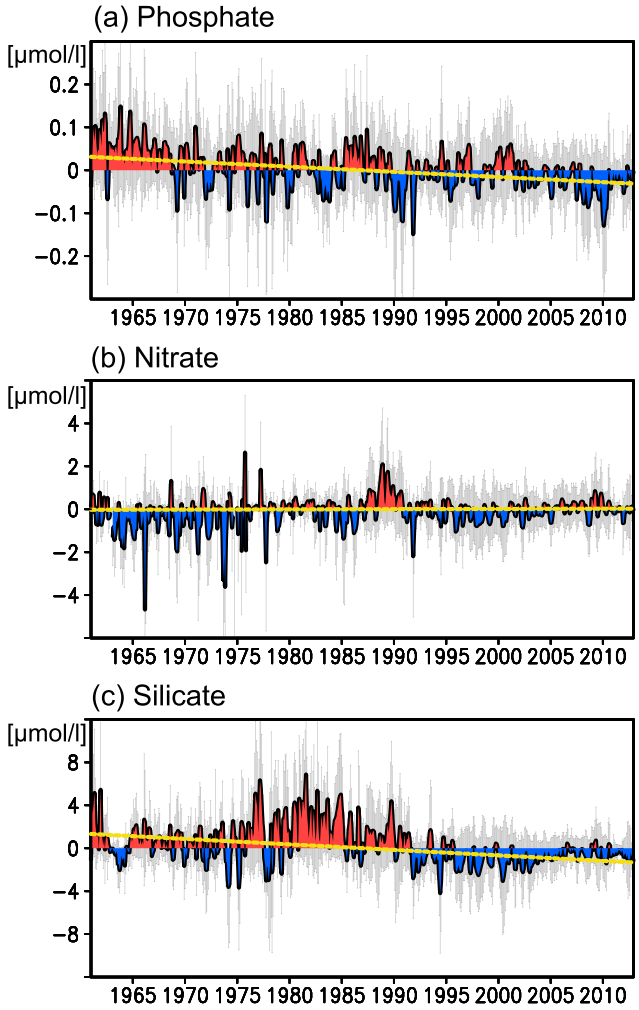

Figure 3. (a) Phosphate, (b) nitrate, and (c) silicate concentration anomalies after subtracting the PDO- and NPGO-related variabilities averaged over the North Pacific (red and blue shadings). Gray error bars denote standard deviations of the averages. The yellow line denotes the regression coefficient of the trend time series averaged over the North Pacific.

Pacific [*Chhak et al.*, 2009]. A mixed layer deepening would induce an increase of nutrient concentrations via enhanced entrainment of subsurface, nutrient-rich water. In addition, stronger westerly winds force more nutrient-rich water southward from higher latitudes (Figure 2f (middle)).

3.3. Long-Term Trends

The 52 year trends of phosphate and silicate concentrations are negative over a wide area of the North Pacific (Figures 2b (right) and 2d (right)). The trends of phosphate are more negative than $-0.02\,\mu\text{mol}\,\text{l}^{-1}\,\text{decade}^{-1}$ in a wide area north of 25°N, except along the 40–45°N latitudinal band, and the trends of silicate are more negative than $-0.4\,\mu\text{mol}\,\text{l}^{-1}\,\text{decade}^{-1}$ in a wide area north of 25°N, except in the northeastern Pacific. In contrast, the nitrate trend is negative only around 50°N, 160°E and is positive in most of the other subarctic regions (Figure 2c (right)). However, regression patterns of the liner trend are slightly different among the sensitivity tests, and the spatial correlations are sometimes insignificant. Nevertheless, the trends averaged over the North Pacific are consistent in each case. That is, the regression patterns of the linear trend are not robust, except for the trends averaged over the North Pacific. We therefore focus here on the trends averaged over the North Pacific. Trends of phosphate and silicate averaged over the North Pacific are $-0.012 \pm 0.005\,\mu\text{mol}\,\text{l}^{-1}\,\text{decade}^{-1}$ and $-0.38 \pm 0.13\,\mu\text{mol}\,\text{l}^{-1}\,\text{decade}^{-1}$, whereas the nitrate trend averaged over the North Pacific is $0.01 \pm 0.12\,\mu\text{mol}\,\text{l}^{-1}\,\text{decade}^{-1}$ (average ± standard error; Figure 3). The inconsistent trend between nitrate and phosphate leads to a positive trend of $N^* (= [NO_2 + NO_3] - R_{N/P}\,[PO_4] + 2.9$, where $R_{N/P} = 16$ [*Deutsch et al.*, 2001]). The N^* trend averaged over the North Pacific is $0.20 \pm 0.21\,\mu\text{mol}\,\text{l}^{-1}\,\text{decade}^{-1}$. Trends in each month are also negative for phosphate and silicate and not significant for nitrate.

Surface ocean density decrease at a rate greater than $0.02\,\text{kg}\,\text{m}^{-3}\,\text{decade}^{-1}$, except for the central to eastern part of the subtropical region (Figure 2e (right)). This density change is a result of a warming of ~0.1°C decade^{-1} and lowering of salinity by ~0.01 decade^{-1}. The surface wind trend is very weak (less than $0.1\,\text{cm}\,\text{s}^{-1}$; Figure 2f (right)). The trends of phosphate and silicate concentrations toward lower values are therefore related to the increasing stratification of the upper ocean.

Here we estimate the reduction of the quantity of nutrients entrained in the upper ocean during the winter by shoaling of the winter mixed layer depth. First, we calculate the climatological means of the vertical density profiles from temperature and salinity in the upper ocean at each grid point. Next, we convert the surface density trend into a long-term trend of mixed layer depth by using the climatological density profiles during summer at the climatological mean MLD in winter from MILA_GPV. As a result, shoaling of the winter MLD is

estimated to be 2.3 ± 0.9 m decade^{-1} (Figure S3a). Our MLD trend estimate is roughly consistent with previous estimates in the western subarctic Pacific (0.3 m yr^{-1}) [*Ono et al.*, 2001] and at Station Papa (50°N, 145°W; 0.63 m yr^{-1}) [*Freeland et al.*, 1997].

Assuming that annual new production is constant (c), we determine the winter nutrient concentration at year $i+1$ (n^{i+1}_w) from the winter nutrient concentration at year i (n^{i}_w), the winter mixed layer depth (h^{i+1}_w), and summer euphotic zone depth (h_s):

$$n^{i+1}{}_w = \left\{\left(n^{i}{}_w - c\right)h_a + \left[a + b\left(h_s + h^{i+1}{}_w\right)/2\right]\left(h^{i+1}{}_w - h_s\right)\right\}/h^{i+1}{}_w \quad (2)$$

[*Freeland et al.*, 1997]. The value of a in equation (2) is the minimum concentration of the climatological mean surface concentration of the nutrient, and b is the vertical gradient of the nutrient concentration, which was obtained from a liner regression of the WOA13 nutrient vertical profile (Figures S3b (left) to S3d (left)). By integrating this equation over 52 years, we are able to obtain the trend of decreasing nutrient concentrations in the region where the mixed layer depth clearly change during a seasonal cycle (roughly north of 30°N; Figures S3b (right) to S3d (right)). The reduction of nutrient concentrations by enhancement of surface stratification occurs especially in the subarctic region, where there is a strong contrast between surface and subsurface nutrient concentrations. We estimate the average rate of change of nutrient concentrations to be -0.014 ± 0.006 μmol l^{-1} decade^{-1} for phosphate, -0.19 ± 0.09 μmol l^{-1} decade^{-1} for nitrate, and -0.45 ± 0.21 μmol l^{-1} decade^{-1} for silicate. We obtain similar rates of change when we use the PACIFICA database to calculate the vertical gradients of the nutrient concentrations. These calculated rates of decline of nutrient concentrations correspond well with the observed rates of decline, with the exception of nitrate.

4. Discussion

The PDO- and NPGO-related changes of nutrient concentrations are interpreted in relation to the PDO- and NPGO-related changes of horizontal advection and vertical mixing, as mentioned in section 3. It means that the PDO and the NPGO not only are the dominant climate variation modes in the North Pacific but also induce significant nutrient variability there.

The PDO-related pattern of nutrient concentrations is consistent with the results of *Yasunaka et al.* [2014]. However, their period of analysis was only 10 years (2001–2010), and their nutrient-gridded data were estimated using physical and biogeochemical parameters such as temperature and salinity. Our results confirm the PDO-related nutrient variability over a longer time period and are based purely on observations of nutrient concentrations themselves. In contrast, the positive signal reported by *Yasunaka et al.* [2014] was more confined along the subarctic-subtropical boundary, probably because their mapping technique was able to reproduce the sharp meridional gradient of nutrient concentrations.

Although the NPGO-related behavior presented in our study is consistent with the positive correlation between the NPGO and modeled nitrate concentrations in the Alaskan gyre shown by *Di Lorenzo et al.* [2009], the positive regression coefficients shown by *Di Lorenzo et al.* [2009] were strictly confined along the coastal region. Their confined coastal signal could be associated with the high concentrations of nitrate in the mean state of their model in the coastal region of the Alaskan gyre. However, such high nitrate concentrations do not appear in our data and in the WOA13 (not shown here).

Trends averaged over the North Pacific in this study are considerably smaller in magnitude than those reported by *Ono et al.* [2008] (-0.08 ± 0.02 μmol l^{-1} decade^{-1} for phosphate and -3.5 ± 0.8 μmol l^{-1} decade^{-1} for silicate). In contrast, our estimates are larger in magnitude than those of *Whitney* [2011], who reported trends in surface nutrients that were insignificant in most cases. The magnitude of our estimated N^* trend is smaller than the trends at several points in the subarctic North Pacific reported by *Watanabe et al.* [2008] (1.2 ± 0.6 μmol l^{-1} decade^{-1}). Differences from other studies may reflect the number of data used and the separation of the linear trend signal from the PDO and NPGO signals in the present study. Simple averages of nutrient concentrations at different locations and different months in the previous studies might also have contaminated the real signals with spatiotemporal biases.

Kim et al. [2014] attributed the increase of nitrate relative to phosphate in the upper ocean to depositions of anthropogenic reactive nitrogen. Global anthropogenic nitrogen depositions in 2000 were estimated to be 54 Tg N yr^{-1} by *Duce et al.* [2008]. If the external input of nitrogen is uniformly distributed in the upper

500 m of the ocean, anthropogenic nitrogen deposition would increase the nitrate concentration by roughly 0.2 μmol l^{-1} decade^{-1}. The order of magnitude of the effect of external nitrogen input is comparable to the mixed layer shoaling effect estimated in this study. However, a reduction of nitrate concentrations due to the mixed layer shoaling effect is apparent in the subarctic (Figure S3c (right)), whereas the effect of nitrogen deposition is prominent in the western North Pacific [*Duce et al*., 2008].

Trends toward higher nutrient concentrations below the surface layer have been observed in recent decades [*Ono et al*., 2001; *Whitney et al*., 2013]. According to *Whitney et al.* [2013], nutrient concentrations in the North Pacific have been increasing at a rate of about 0.2 mmol m^{-2} yr^{-1} for phosphate, 16 mmol m^{-2} yr^{-1} for nitrate, and 24 mmol m^{-2} yr^{-1} for silicate between the bottom of the winter mixed layer and a depth of 1000 m. If the winter mixed layer is 100 m deep, these increases of subsurface nutrient concentrations would have been canceled out by decreases of 0.02 μmol l^{-1} decade^{-1} for phosphate, 1.6 μmol l^{-1} decade^{-1} for nitrate, and 2.4 μmol l^{-1} decade^{-1} for silicate. However, the surface trends detected in the present study are much smaller than these rates, as discussed by *Whitney et al.* [2013].

5. Concluding Remarks

By using extensive ocean surface nutrient concentration data, we elucidated the spatial patterns of the nutrient concentration variabilities through changes in horizontal advection and vertical mixing related to the PDO and the NPGO. We also determined surface trends of phosphate and silicate averaged over the North Pacific that corresponded well with the effect of shoaling of the mixed layer.

To our knowledge, this is the first report of the spatial distributions and temporal changes of the long-term variability of surface nutrient concentrations based on measured nutrient concentrations themselves. The fact that the dominant climate variations (PDO, NPGO, and long-term trend) affect ocean nutrient concentrations has an important implication for understanding biogeochemical changes under global warming. In addition, our optimally interpolated data sets (available at http://www.jamstec.go.jp/res/ress/yasunaka/nutrient/) are useful validation data for ocean biogeochemical and Earth system models and should facilitate development of the models.

Robust spatial distributions of the trends of nutrient concentrations were not obtained in the present study. Further observations over a wide area and for a long period of time will be necessary to clarify the trends. Seasonal changes of PDO- and NPGO-related patterns and the long-term trends are important subjects because they are closely related to long-term changes of biological production, and they will be a subject of our future work.

Acknowledgments
The NIES Volunteer Observing Ship program has been conducted with the cooperation of the Seaboard International Shipping Co., the Mitsui O.S.K. Lines Co., the Toyofuji Shipping Co., and the Kagoshima Senpaku Co. We gratefully acknowledge the support and collection of water samples by the captain, officers, crews, and observers on board the M/S *Skaugran*, M/S *Alligator Hope*, M/S *Pyxis*, and M/S *Trans Future 5*, and the assistance of S. Kariya, T. Yamada, and J. Yamamura of the Global Environmental Forum. We thank R. Bellegay and M. Davelaar of Fisheries and Oceans Canada for their assistance with the observations, and M. Uematsu, M. Shigemitu, and two anonymous reviewers for providing useful comments. This work was financially supported by a Grant-in-Aid for Scientific Research on Innovative Areas and the Global Environment Research Account for National Institutes by the Ministry of Environment, Japan. The NIES and IOS nutrient data are available from the authors upon request (nakaoka.shinichiro@nies.go.jp; whitneyf@shaw.ca). JAMSTEC monitoring data are distributed by JAMSTEC (http://www.godac.jamstec.go.jp/darwin/explain/81/e). PACIFICA, the Line P data, and WOD13 are available online (http://cc-s.pices.jp/; https://www.waterproperties.ca/linep/index.php; http://www.nodc.noaa.gov/OC5/WOD/pr_wod.html). The temperature and salinity data of *Ishii and Kimoto* [2009] were obtained from the Research Data Archive at the National Center for Atmospheric Research (http://rda.ucar.edu/datasets/ds285.3/#!description).

References

Bopp, L., P. Monfray, O. Aumont, J.-L. Dufresne, H. Le Treut, G. Madec, L. Terray, and J. C. Orr (2001), Potential impacts of climate change on marine export production, *Global Biogeochem. Cycles*, *15*, 81–99, doi:10.1029/1999GB001256.

Boyer, T. P., et al. (2013), World ocean database 2013, Sydney Levitus, Ed.; Alexey Mishonov, Technical Ed.; NOAA Atlas NESDIS 72, 209 pp.

Cayan, D. (1992), Latent and sensible heat flux anomalies over the northern oceans: The connection to monthly atmospheric circulation, *J. Clim.*, *5*, 354–369.

Chhak, K. C., E. Di Lorenzo, N. Schneider, and P. F. Cummins (2009), Forcing of Low-frequency ocean variability in the northeast Pacific, *J. Clim.*, *22*, 1255–1276, doi:10.1175/2008JCLI2639.1.

Deutsch, C., N. Gruber, R. M. Key, J. L. Sarmiento, and A. Ganachaud (2001), Denitrification and N2 fixation in the Pacific Ocean, *Global Biogeochem. Cycles*, *15*(2), 483–506, doi:10.1029/2000GB001291.

Di Lorenzo, E., et al. (2008), North Pacific Gyre Oscillation links ocean climate and ecosystem change, *Geophys. Res. Lett.*, *35*, L08607, doi:10.1029/2007GL032838.

Di Lorenzo, E., et al. (2009), Nutrient and salinity decadal variations in the central and eastern North Pacific, *Geophys. Res. Lett*, *36*, L14601, doi:10.1029/2009GL038261.

Duce, R. A., et al. (2008), Impacts of atmospheric anthropogenic nitrogen on the open ocean, *Science*, *320*, 893–897.

Fisheries and Oceans Canada (2012), [Available at http://www.pac.dfo-mpo.gc.ca/science/oceans/data-donnees/line-p/index-eng.html.]

Freeland, H., K. Denman, C. S. Wong, F. Whitney, and R. Jacques (1997), Evidence of change in the winter mixed layer in the northeast Pacific Ocean, *Deep Sea Res., Part I*, *44*(12), 2117–2129.

Garcia, H. E., R. A. Locarnini, T. P. Boyer, J. I. Antonov, O. K. Baranova, M. M. Zweng, J. R. Reagan, and D. R. Johnson (2014), World ocean atlas 2013, volume 4: Dissolved inorganic nutrients (phosphate, nitrate, silicate), S. Levitus, Ed., A. Mishonov Technical Ed.; NOAA Atlas NESDIS 76, 25 pp.

Hosoda, S., T. Ohira, and T. Nakamura (2008), A monthly mean dataset of global oceanic temperature and salinity derived from Argo float observations, *JAMSTEC Rep. Res. Dev.*, *8*, 47–59.

Hosoda, S., T. Ohira, K. Sato, and T. Suga (2010), Improved description of global mixed-layer depth using Argo profiling floats, *J. Oceanogr.*, *66*, 773–787.

Ishii, M., and M. Kimoto (2009), Reevaluation of historical ocean heat content variations with time-varying XBT and MBT depth bias corrections, *J. Oceanogr.*, *65*, 287–299.
Kalnay, E., et al. (1996), The NCEP/NCAR 40-year reanalysis project, *Bull. Am. Meteorol. Soc.*, *77*, 437–471.
Kim, I. N., K. Lee, N. Gruber, D. M. Karl, J. L. Bullister, S. Yang, and T. W. Kim (2014), Chemical oceanography. Increasing anthropogenic nitrogen in the North Pacific Ocean, *Science*, *346*, 1102–1106, doi:10.1126/science.1258396.
Kim, T. W., K. Lee, R. G. Najjar, H. D. Jeong, and H. J. Jeong (2011), Increasing N abundance in the northwestern Pacific Ocean Due to atmospheric nitrogen deposition, *Science*, *334*, 505–509, doi:10.1126/science.1206583.
Lee, Z., A. Weidemann, J. Kindle, R. Arnone, K. L. Carder, and C. Davis (2007), Euphotic zone depth: Its derivation and implication to ocean-color remote sensing, *J. Geophys. Res.*, *112*, C03009, doi:10.1029/2006JC003802.
Mantua, N. J., S. R. Hare, Y. Zhang, J. M. Wallace, and R. C. Francis (1997), A Pacific interdecadal climate oscillation with impacts on salmon production, *Bull. Am. Meteorol. Soc.*, *78*, 1069–1079.
Miller, A. J., D. R. Cayan, T. P. Barnett, N. E. Graham, and J. M. Oberhuber (1994), Interdecadal variability of the Pacific Ocean: Model response to observed heat flux and wind stress anomalies, *Clim. Dyn.*, *9*, 287–302.
Ono, T., T. Midorikawa, Y. W. Watanabe, K. Tadokoro, and T. Saino (2001), Temporal increases of phosphate and apparent oxygen utilization in the subsurface waters of western subarctic Pacific from 1968 to 1998, *Geophys. Res. Lett.*, *28*, 3285–3288, doi:10.1029/2001GL012948.
Ono, T., K. Tadokoro, T. Midorikawa, J. Nishioka, and T. Saino (2002), Multi-decadal decrease of net community production in western subarctic North Pacific, *Geophys. Res. Lett.*, *29*(8), 1186, doi:10.1029/2001GL014332.
Ono, T., A. Shiomoto, and T. Saino (2008), Recent decrease of summer nutrients concentrations and future possible shrinkage of the subarctic North Pacific high-nutrient low-chlorophyll region, *Global Biogeochem. Cycles*, *22*, GB3027, doi:10.1029/2007GB003092.
Peña, M. A., and D. E. Varela (2007), Seasonal and interannual variability in phytoplankton and nutrient dynamics along line P in the NE subarctic Pacific, *Prog. Oceanogr.*, *75*, 200–222.
Suzuki, T., et al. (2013), *PACIFICA Data Synthesis Project. ORNL/CDIAC-159, NDP-092. Carbon Dioxide Information Analysis Center*, Oak Ridge National Laboratory, U.S. Department of Energy, Oak Ridge, Tenn., doi:10.3334/CDIAC/OTG.PACIFICA_NDP092.
Watanabe, Y. W., M. Shigemitsu, and K. Tadokoro (2008), Evidence of change in oceanic fixed nitrogen with decadal climate change in the North Pacific subpolar region, *Geophys. Res. Lett.*, *35*, L01602, doi:10.1029/2007GL032188.
Whitney, F. A. (2011), Nutrient variability in the mixed layer of the subarctic Pacific Ocean, 1987–2010, *J. Oceanogr.*, *67*, 481–492.
Whitney, F. A., S. Bograd, and T. Ono (2013), Nutrient enrichment of the subarctic Pacific Ocean pycnocline, *Geophys. Res. Lett.*, *40*, 2200–2205, doi:10.1002/grl.50439.
Woods, J., and W. Barkmann (1993), Diatom demography in winter—Simulated by the Lagrangian Ensemble method, *Fish. Oceanogr.*, *2*, 202–222, doi:10.1111/j.1365-2419.1993.tb00136.x.
Yasunaka, S., Y. Nojiri, S. Nakaoka, T. Ono, F. A. Whitney, and M. Telszewski (2014), Mapping of sea surface nutrients in the North Pacific: Basin-wide distribution and seasonal to interannual variability, *J. Geophys. Res. Oceans*, *119*, 7756–7771, doi:10.1002/2014JC010318.